Xavier del Toro Garcia, Antoni Arias, Marcel G. Jayne, Phil A. Witting, Vicenç M. Sala, Jose Luis Romeral

New DTC Control Scheme for Induction Motors fed with a Three-level Inverter

Original scientific paper

This paper presents a novel controller based on Direct Torque Control (DTC) strategy. This controller is designed to be applied in the control of Induction Motors (IM) fed with a three-level Voltage Source Inverter (VSI). This type of inverter has several advantages over the standard two-level VSI, such as a greater number of levels in the output voltage waveforms, lower dV/dt, less harmonic distortion in voltage and current waveforms and lower switching frequencies. In the new controller, torque and stator flux errors are used together with the stator flux angular frequency to generate a reference voltage vector. Experimental results of the novel system are presented and compared with those obtained for Classical DTC system employing a two-level VSI. The new controller is shown to reduce the ripple in the torque and flux responses. Lower current distortion and switching frequency of the semiconductor devices are also obtained in the new system presented.

Key words: adjustable speed drives, direct torque and flux control, induction motors, multilevel converters

1 INTRODUCTION

Direct Torque Control (DTC) is a method that has emerged to become one possible alternative to the well-known Vector Control of Induction Motors [1–3]. This method provides a good performance with a simpler structure and control diagram. In DTC it is possible to control directly the stator flux and the torque by selecting the appropriate VSI state. The main advantages offered by DTC are:

– Decoupled control of torque and stator flux.

– Excellent torque dynamics with minimal response time.

– Inherent motion-sensorless control method since the motor speed is not required to achieve the torque control.

– Absence of coordinate transformation (required in Field Oriented Control (FOC)).

– Absence of voltage modulator, as well as other controllers such as PID and current controllers (used in FOC).

– Robustness for rotor parameters variation. Only the stator resistance is needed for the torque and stator flux estimator.

These merits are counterbalanced by some drawbacks:

– Possible problems during starting and low speed operation and during changes in torque command.

– Requirement of torque and flux estimators, implying the consequent parameters identification (the same as for other vector controls).

– Variable switching frequency caused by the hysteresis controllers employed.

– Inherent torque and stator flux ripples.

– Flux and current distortion caused by sector changes of the flux position.

– Higher harmonic distortion of the stator voltage and current waveforms compared to other methods such as FOC.

– Acoustical noise produced due to the variable switching frequency. This noise can be particularly high at low speed operation.

A variety of techniques have been proposed to overcome some of the drawbacks present in DTC [4]. Some solutions proposed are: DTC with Space Vector Modulation (SVM) [5]; the use of a duty-ratio controller to introduce a modulation between active vectors chosen from the look-up table and the zero vectors [6–8]; use of artificial intelligence techniques, such as Neuro-Fuzzy controllers with SVM [9]. These methods achieve some improvements such as torque ripple reduction and fixed switching frequency operation. However, the complexity of the control is considerably increased.

A different approach to improve DTC features is to employ different converter topologies from the standard two-level VSI. Some authors have presen-

ted different implementations of DTC for the three-level Neutral Point Clamped (NPC) VSI [10–15]. This work will present a new control scheme based on DTC designed to be applied to an Induction Motor fed with a three-level VSI. The major advantage of the three-level VSI topology when applied to DTC is the increase in the number of voltage vectors available. This means the number of possibilities in the vector selection process is greatly increased and may lead to a more accurate control system, which may result in a reduction in the torque and flux ripples. This is of course achieved, at the expense of an increase in the complexity of the vector selection process.

2 THE THREE-LEVEL NPC INVERTER

The standard VSI traditionally used in electrical drive systems is the two-level VSI, which unfortunately has a number of inherent limitations. For example the maximum voltage that can be supported by the semiconductor switching devices in the inverter limits the maximum value of DC bus voltage. Similarly the output voltages and currents from the inverter can contain high harmonic distortion. The output voltage waveforms can also contain large values of dV/dt, which contribute to the degradation of the machine windings insulation and also produce considerable electromagnetic interference during operation. New multilevel VSI topologies however can considerably reduce many of these limitations [16].

The three-level NPC VSI, presented in Figure 1, is one of the most commonly applied multilevel topologies [17]. This type of VSI has several advantages over the standard two-level VSI, such as a greater number of levels in the output voltage waveforms, lower dV/dt, less harmonic distortion and lower switching frequencies. The main drawback of this type of converter is the voltage imbalance produced in the capacitors of the DC-link
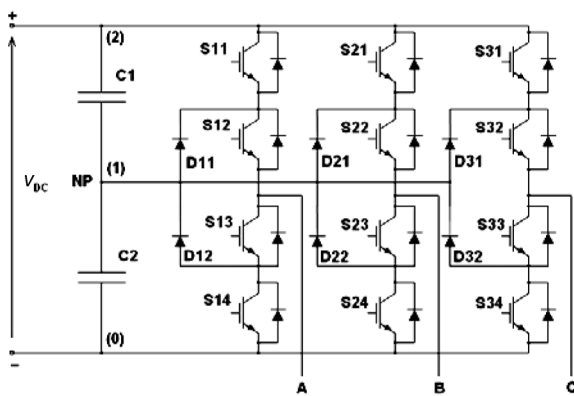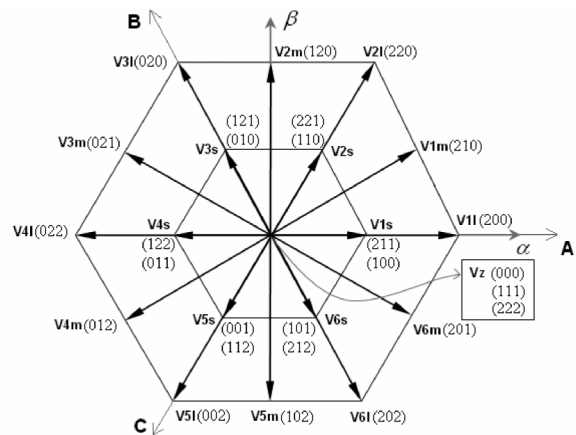

Fig. 1 Three-level NPC VSI

Fig. 2 Voltage space vectors for a three-level NPC VSI

when one of the phases is connected to the middle point or Neutral Point (NP).

In Figure 2, the different vectors or VSI states available in a three-level VSI are presented. As it can be seen, there are 4 different kinds of vectors depending on the module:

–   Zero vectors: Vz (with 3 possible configurations).

–   Large vectors: V1l, V2l, V3l, V4l, V5l, V6l.

–   Medium vectors: V1m, V2m, V3m, V4m, V5m, V6m.

–   Small vectors: V1s, V2s, V3s, V4s, V5s, V6s. (with 2 possible configurations for each).

The state of the switches for each leg (C_A, C_B and C_C) is shown in brackets (2: phase connected to the positive of the DC-link; 1: phase connected to the middle point of the DC-link (NP); 0: phase connected to the negative of the DC-link). The output voltage vector is defined by the following expression:

$$\vec{v} = \frac{V_{DC}}{9}(3C_A + bC_B + b^*C_C); \quad C_A, C_B, C_C \in \{0,1,2\}$$

(1)

where $a = e^{j\frac{2\pi}{3}}$ and $b = 2a - a^2 - 1$.

3 DTC PRINCIPLE REVIEW

In order to understand DTC principle some of the equations of the Induction Motor need to be reviewed. The electromagnetic torque can be expressed as a function of the stator flux and the rotor flux space vectors as follows:

$$\Gamma_e = -\frac{3}{2}P\frac{L_m}{L_sL_r - L_m^2}\vec{\psi}_s \times \vec{\psi}_r'.$$

(2)

If the modulus of the previous expression is evaluated it is obtained:

$$\Gamma_e = \frac{3}{2} P \frac{L_m}{L_s L_r - L_m^2} \left| \vec{\psi}_r' \right| \left| \vec{\psi}_s \right| \sin\left(\gamma_s - \gamma_r \right). \qquad (3)$$

Considering the modulus of the rotor and stator fluxes constant, torque can be controlled by changing the relative angle between both flux vectors. Stator flux can be adjusted by the stator voltage according to the stator voltage equation in stator fixed coordinates:

$$\vec{u}_s = R_s \vec{i}_s + \frac{d\vec{\psi}_s}{dt}. \qquad (4)$$

If the voltage drop in the stator resistance is neglected the variation of the stator flux is directly proportional to the stator voltage applied:

$$\vec{u}_s \quad \frac{d\vec{\psi}_s}{dt} \qquad \vec{u}_s \quad \frac{\Delta\vec{\psi}_s}{\Delta t}. \qquad (5)$$

Because the rotor time constant is larger than the stator one, the rotor flux changes slowly compared to the stator flux. Thus torque can be controlled by quickly varying the stator flux position by means of the stator voltage applied to the motor. The desired decoupled control of the stator flux modulus and torque is achieved by acting on the radial (x) and tangential (y) components respectively of the stator flux vector. According to (5) these two components will depend on the components of the stator voltage vector applied in the same directions. The tangential component of the stator voltage will affect the relative angle between the rotor and the stator flux vectors and in turns will control the torque variation according to (3). The radial component will affect the amplitude of the stator flux vector.

Figure 3 shows the stator flux in the α-β plane, and the effect of the different states of a two-level
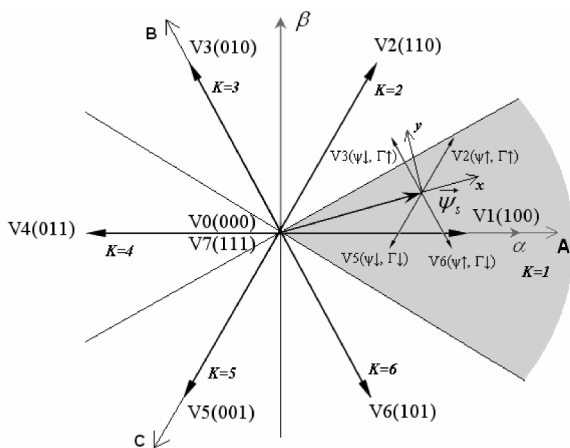

Fig. 3 Influence of the voltage vector selected on the variation of stator flux modulus and torque

VSI regarding torque and stator flux modulus variation. The α-β plane is divided into six different sectors. As an example, for sector 1 ($K = 1$), V2 can increase both stator flux and torque.

According to the considerations illustrated in Figure 3 the generic or Classical DTC scheme for a VSI-fed Induction Motor was developed [1] as shown in Figure 4.
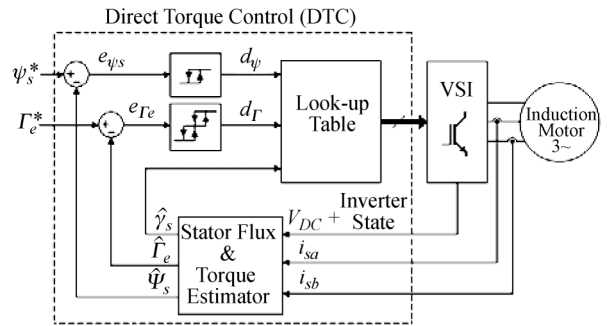

Fig. 4 Classical DTC scheme

As it can be seen, there are two different loops corresponding to the magnitudes of the stator flux modulus and torque. The reference values for the stator flux modulus and the torque are compared with the estimated values, the resulting error values are fed into a two-level and a three-level hysteresis block respectively. The outputs of the stator flux error and torque error hysteresis blocks, together with the position of the stator flux are used as inputs to the look-up table (Table 1). The position of the stator flux is divided into six different sectors. The output of the look-up table is the VSI state that will be applied during a sampling period. The stator flux modulus and torque errors tend to be restricted within its respective hysteresis bands.

The principle of DTC operation can also be explained by analysing the Induction Motor stator voltage equation in the stator flux reference frame.

$$\vec{u}_s = R_s \vec{i}_s + \frac{d\vec{\psi}_s}{dt} + j\omega_s \vec{\psi}_s. \qquad (6)$$

Table 1 **Classical DTC look-up table**

$K(\gamma_s)$		1	2	3	4	5	6
$d_\psi = 1$	$d_\Gamma = 1$	V2	V3	V4	V5	V6	V1
	$d_\Gamma = 0$	V7	V0	V7	V0	V7	V0
	$d_\Gamma = -1$	V6	V1	V2	V3	V4	V5
$d_\psi = -1$	$d_\Gamma = 1$	V3	V4	V5	V6	V1	V2
	$d_\Gamma = 0$	V0	V7	V0	V7	V0	V7
	$d_\Gamma = -1$	V5	V6	V1	V2	V3	V4

If this expression is separated into de direct (x) and the quadrature component (y) of the stator voltage, the following expressions are can be obtained:

$$u_{sx} = R_s i_{sx} + \frac{d\psi_{sx}}{dt} \qquad (7)$$

$$u_{sy} = R_s i_{sy} + \omega_s \psi_{sx}. \qquad (8)$$

In the same reference frame fixed to the stator flux vector the electromagnetic torque can be expressed as:

$$\Gamma_e = \frac{3}{2} P \vec{\psi}_s \times \vec{i}_s \qquad (9)$$

$$\Gamma_e = \frac{3}{2} P(\psi_{sx} i_{sy} - \psi_{sy} i_{sx}) = \frac{3}{2} P \psi_{sx} i_{sy}. \qquad (10)$$

Combining expression (8) with (10) the following torque expression is obtained:

$$\Gamma_e = \frac{3}{2} P \frac{\psi_{sx}(u_{sy} - \omega_s \psi_{sx})}{R_s}. \qquad (11)$$

From expression (7) it can be concluded that stator flux amplitude can be controlled by means of the direct (or radial) component of the stator voltage. It is also evident from equation (11) that the electromagnetic torque can be controlled by means of the quadrature (or tangential) component of the stator voltage, under adequate decoupling of the stator flux. From equation (11) some other considerations can be made:

– Torque depends on the stator flux amplitude as well.

– It also depends on the stator flux angular speed, which depends on the operating point of the machine. It can be seen that as the speed of the machine and the slip increase the effect of the voltage vectors applied on the produced torque is lower. It is also obvious that zero vectors will produce a high torque decrease at high speeds.

DTC requires the estimation of stator flux and torque, which can be performed by means of two different phase currents, the state of the VSI and the voltage level in the DC-link. This estimation is based in the stator voltage equation [3]:

$$\vec{\psi}_s = \int (\vec{u}_s - R_s \vec{i}_s) \, dt. \qquad (12)$$

Torque expression is then obtained using (9).

4 NEW DTC SCHEME

In the new controller, shown in Figure 5, a reference voltage vector (V_{ref}) in α-β coordinates is generated according to the DTC basic principle explained in the previous section, rather than using
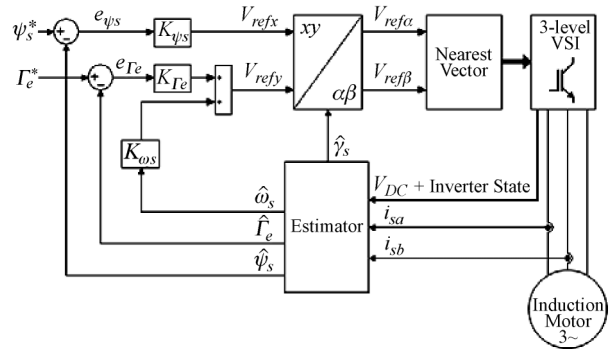

Fig. 5 New DTC scheme

the inverter state look-up table as used in classical DTC. This approach adopted is close to the DTC with Space Vector Modulation (SVM) scheme with closed-loop flux and torque control, and Stator Flux Oriented Control [4]. The inputs to the controller are the stator flux error, the torque error and additionally the stator flux angular speed, which is incorporated to improve the torque response at different operating points. The reference voltage generated as a control action can be synthesised using different techniques with different degrees of complexity such as choosing the nearest vector available or using modulation techniques. This controller can be applied to any topology because the type of VSI will only affect the way the reference voltage vector has to be synthesised.

Following the conclusions extracted from (7) and (11), when calculating the reference voltage (in x-y coordinates fixed to the stator flux vector) the radial or x component will depend on the stator flux error, while the tangential or y component will depend on the torque error. A feed-forward action depending on the stator flux angular speed is added in the calculation of the stator voltage y component. This action will compensate the effect of the operating point on the torque production. Initially a preliminary reference vector in x-y coordinates is calculated; where some gain factors have been introduced to tune the controller.

$$V_{refx} = K_{\psi s} e_{\psi s} \qquad (13)$$

$$V_{refy} = K_{\Gamma e} e_{\Gamma e} + K_{\omega s} \hat{\omega}_s. \qquad (14)$$

Then a transformation x-y to α-β is performed to obtain the reference vector in fixed coordinates. In this point, the new controller synthesises the reference voltage vector by choosing the nearest vector available that can be delivered by the VSI. The nearest vector is found by means of calculating the minimum distance of the voltage vectors that can be delivered by the VSI to the reference voltage vector.
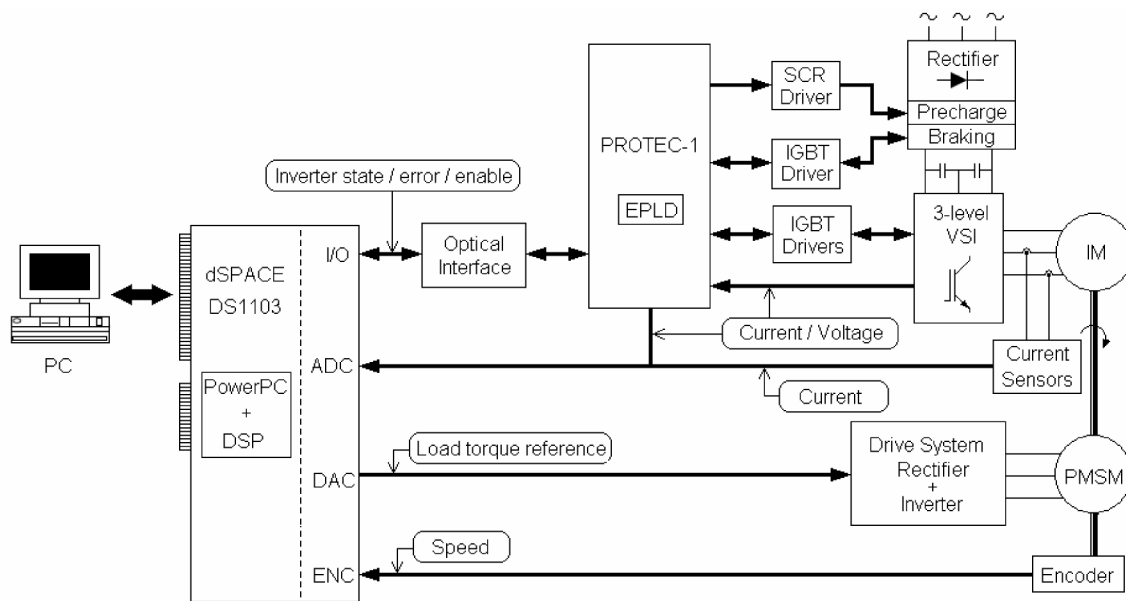
Fig. 6 Experimental setup

A different possibility instead of choosing the nearest vector and applying it for the whole sampling period is to use modulation techniques such as Space Vector Modulation (SVM) or some active-null vector modulation like in a duty-ratio controller. These possibilities will also provide a higher but constant switching frequency.

5 EXPERIMENTAL SETUP

The novel controller has been tested in an experimental setup. This setup contains the following components as shown in Figure 6:

– A dSpace DS1103 board that performs the control tasks. This board contains a PowerPC and a DSP.

– A 30 A three-level NPC VSI with Insulated Gate

Table 2 **Induction Motor parameters**

Rated power	1.1 kW (Y: 380 V/4.43 A)
Poles	4
Nominal speed	1415 rpm = 148.17 rad/s
Nominal torque	7.4 Nm
Nominal Flux	0.96 Wb
R_s	9.21 Ω
R_r	6.644 Ω
L_m	0.44415 H
L_s	0.03207 H
L_r	0.00847 H

Bipolar Transistors (IGBT) to supply an Induction Motor.

– A 1.1 kW Induction Motor to be controlled. Table 2 shows the parameters of this motor.

– A permanent magnet synchronous motor (PMSM) attached to the Induction Motor shaft and supplied with an industrial rectifier and inverter. Torque load can be controlled with this equipment by sending the load torque reference signal from the control board.

– The control algorithm has been created using Matlab/Simulink.

6 EXPERIMENTAL RESULTS

Some experimental results have been obtained for the Classical DTC control system with a two-level VSI (DTC2L) and the new control technique with a three-level VSI (NDTC3L) to establish a comparison between both systems. Figure 7 and Figure 8 show the torque response, stator flux response and stator currents at 50 rpm and no load conditions for both systems respectively. Figure 9 and Figure 10 show the torque response, stator flux response and stator currents at 200 rpm and nominal torque conditions (7.4 Nm) for both systems respectively.

The sample time used in the control system is 100 μs. In order to assess the performance of both systems, the torque standard deviation and stator flux standard deviation are calculated to evaluate the ripple of both variables. The expression for the standard deviation of a generic variable employed is as follows (being n the number of samples):
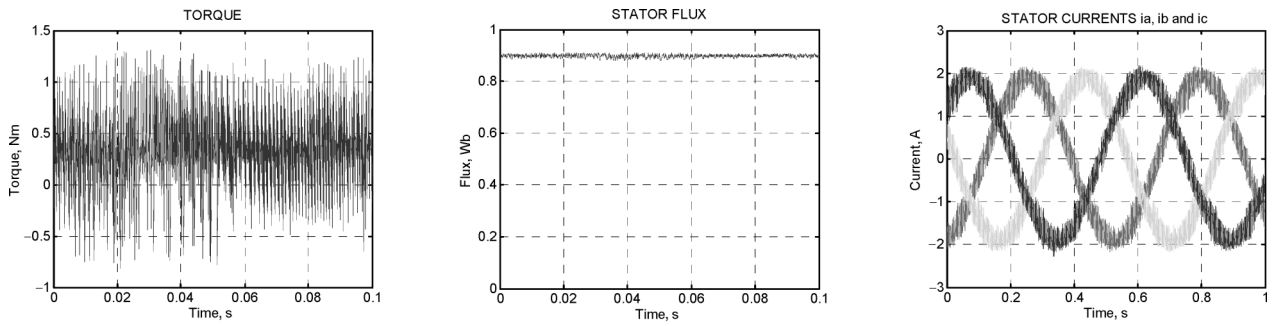
Fig. 7 Torque response (left), stator flux response (centre) and stator currents (right) for DTC2L at 50 rpm and no load
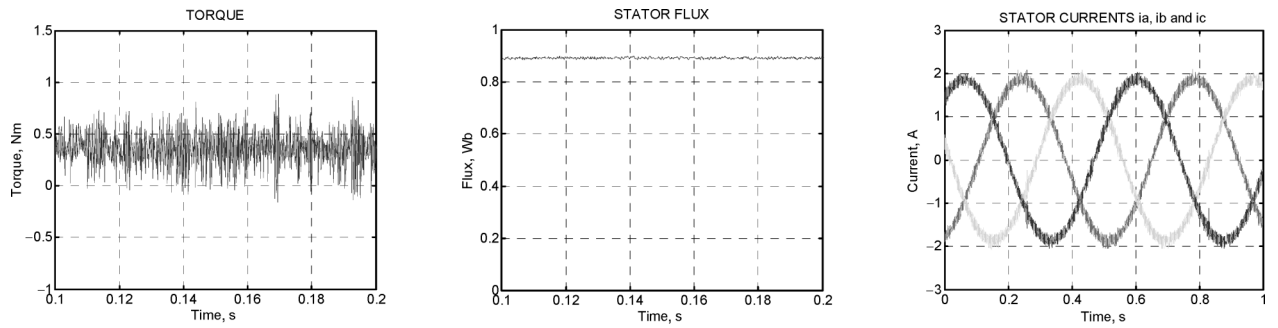

Fig. 8 Torque response (left), stator flux response (centre) and stator currents (right) NDTC3L at 50 rpm and no load
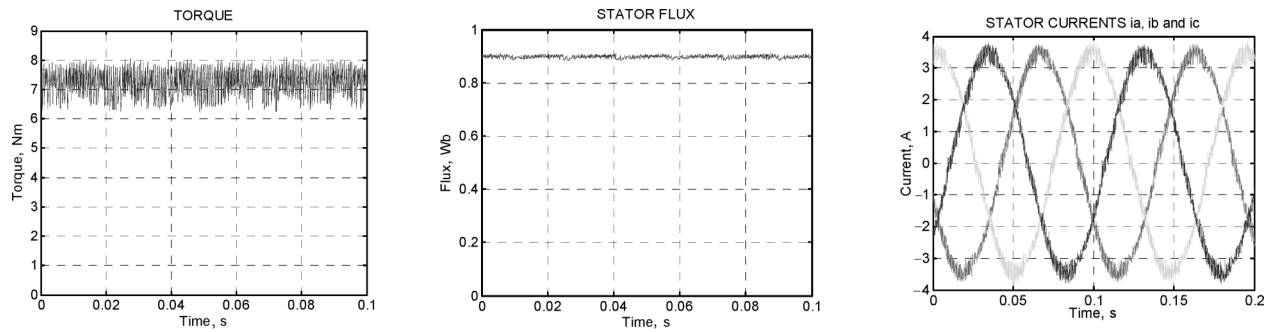

Fig. 9 Torque response (left), stator flux response (centre) and stator currents (right) for DTC2L at 200 rpm and nominal load
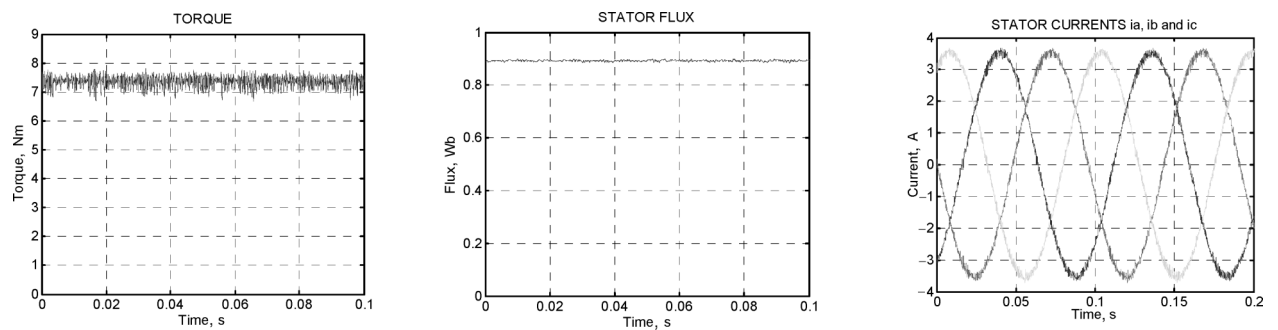

Fig. 10 Torque response (left), stator flux response (centre) and stator currents (right) for NDTC3L at 200 rpm and nominal load

Table 3 **Use of the different types of vector in the NDTC3L system**

Operating point	% zero vectors	% small vectors	% medium vectors	% large vectors
50 rpm and no load	49.52	49.17	1.28	0.04
200 rpm and nominal load	12.51	40.57	26.6	21.32
50 rpm and nominal load	11.85	37.07	28.79	22.31
600 rpm and no load	0.06	9.74	50.08	40.12

$$\sigma = \left(\frac{1}{n-1} \sum_{i=1}^{n} (x_i - \overline{x})^2 \right)^{1/2} \qquad \overline{x} = \frac{1}{n} \sum_{i=1}^{n} x_i. \quad (15)$$

Additionally the Total Harmonic Distortion (THD) of the stator current is calculated and the mean switching frequency of the inverter IGBT devices has been obtained for both systems. These results are shown in Table 4, where two additional operating points are incorporated: 50 rpm and nominal load, and 600 rpm with no load.

From the experimental results presented in Figure 7 to Figure 10 it is apparent that the torque and flux ripple for the new system utilising a three-level

Table 4 **Summary of the experimental results at different operating points**

50 rpm and no load		
SYSTEM	DTC2L	NDTC3L
Torque Standard Deviation	0.44 Nm	0.17 Nm
Flux Standard Deviation	0.0065 Wb	0.003 Wb
Stator current THD	11.89 %	5.07 %
Mean Switching Frequency	6350 Hz	1380 Hz
200 rpm and nominal load		
SYSTEM	DTC2L	NDTC3L
Torque Standard Deviation	0.46 Nm	0.22 Nm
Flux Standard Deviation	0.0059 Wb	0.0029 Wb
Stator current THD	2.62 %	1.17 %
Mean Switching Frequency	4078 Hz	1977 Hz
50 rpm and nominal load		
SYSTEM	DTC2L	NDTC3L
Torque Standard Deviation	0.45 Nm	0.34 Nm
Flux Standard Deviation	0.0059 Wb	0.0027 Wb
Stator current THD	3.20 %	2.04 %
Mean Switching Frequency	5484 Hz	3090 Hz
600 rpm and no load		
SYSTEM	DTC2L	NDTC3L
Torque Standard Deviation	0.30 Nm	0.13 Nm
Flux Standard Deviation	0.0091 Wb	0.0028 Wb
Stator current THD	6.58 %	1.43 %
Mean Switching Frequency	1869 Hz	940 Hz

VSI is considerably reduced. Stator current waveforms also show less distortion for the new system. Measurements made on the results obtained (see Table 4) also show that the THD of the stator currents and the switching frequency of the inverter switches in the proposed system can be both reduced by more than 50 %. Switching frequency is reduced due to the utilisation of a three-level VSI topology. In this type of inverter some transitions between the three possible states of a leg do not involve the commutation of all the semiconductors of the leg. With the new proposed system, NDTC3L, a higher efficiency can be achieved due to the reduction of switching frequencies and THD. This feature together with the improved torque control makes this system an interesting alternative in applications such as electrical vehicles [18].

In Table 3 it is shown the percentage of utilisation for every different type of vector that can be delivered by the three-level VSI at different operating points. It is interesting to see how the small and medium vectors, which do not exist in the two--level topology, play an important role in reducing the torque ripples. This is particularly important for small vectors at low speed and low load operation. It can be seen that in this condition (50 rpm and no load) medium and large vectors are hardly ever employed.
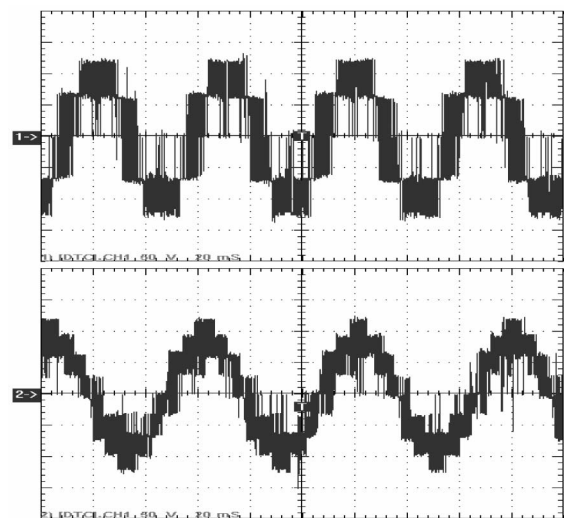

Fig. 11 *Stator phase voltage for DTC2L (up) and NDTC3L (down)*

Finally, in Figure 11 it can be seen the stator voltage waveforms captured with the oscilloscope in the star-connected motor phases. The number of voltage levels delivered by the two-level VSI is 5, while in the case of the three level VSI this number is increased to 9 voltage levels, achieving a more sinusoidal and motor-friendly waveform. It is evident that voltage dV/dt is reduced with the three-level VSI.

7 CONCLUSIONS

A novel controller based on the DTC principle is presented and it is shown that it can be easily implemented in a three-level VSI drive system. The inputs of the controller are the stator flux error, the torque error and additionally the stator flux angular speed. A reference voltage vector is then generated instead of choosing the inverter state through a look-up table as in the Classical DTC system. The reference voltage generated at the output of the controller is then synthesised applying the nearest vector available. This controller can be easily applied to different VSI topologies. The novel controller equations do not involve the use of motor parameters. Motor parameters are only used in the inherent torque and stator flux estimation necessary in any DTC system. The experimental results obtained for the new DTC scheme with a three-level VSI illustrate a considerable reduction in torque ripple, flux ripple, harmonic distortion in stator currents and switching frequency when compared to the existing Classical DTC system utilising two-level VSI.

LIST OF SYMBOLS

Γ_e – electromagnetic torque
Γ_e^* – torque reference
$\hat{\Gamma}_e$ – estimated torque
$e_{\Gamma e}$ – torque error
d_Γ – torque error label
$\vec{\psi}_s$ – stator flux vector
ψ_{sx} – x component of the stator flux vector
ψ_{sy} – y component of the stator flux vector
ψ_e^* – stator flux module reference
$\hat{\psi}_s$ – estimated stator flux
$\hat{\gamma}_s$ – estimated stator flux angle
ω_s – stator flux angular speed
$\hat{\omega}_s$ – estimated stator flux angular speed
$e_{\psi s}$ – stator flux error
K – stator flux sector position
d_ψ – stator flux error label

P – pole pairs
L_m – magnetising inductance
L_s – stator inductance
L_r – rotor inductance
R_s – stator resistance
R_r – rotor resistance
$\vec{\psi}_r'$ – rotor flux vector referred to the stator
$\vec{u}_s$ – stator voltage vector
u_{sx} – x component of the stator voltage vector
u_{sy} – y component of the stator voltage vector
$\vec{i}_s$ – stator current vector
i_{sx} – x component of the stator current vector
i_{sy} – y component of the stator current vector
i_{sa} – stator current phase a
i_{sb} – stator current phase b
V_{DC} – DC-link voltage
V_{refx} – x component of the voltage reference
V_{refy} – y component of the voltage reference
$V_{ref\alpha}$ – α component of the voltage reference
$V_{ref\beta}$ – β component of the voltage reference
$K_{\Gamma e}$ – torque gain
$K_{\psi s}$ – stator flux gain
$K_{\omega s}$ – stator flux angular speed gain.

REFERENCES

[1] I. Takahashi, T. Noguchi, **A New Quick-response and High-efficiency Control Strategy of an Induction Motor.** IEEE Transactions on Industrial Applications, Vol. IA-22, no. 5, pp. 820–827, 1986.

[2] M. Depenbrock, **Direct Self Control of Inverter-fed Induction Machines**. IEEE Transactions in Power Electronics, Vol. PE-3, no. 4, pp. 420–429, Oct. 1988.

[3] ..., ABB. **Direct Torque Control – the World's Most Advanced AC Drive Technology.** Technical guide no. 1, 1999.

[4] G. Buja, M. P. Kazmierkowski, **Direct Torque Control of PWM Inverter-Fed AC Motors – A Survey.** IEEE Transactions on Industrial Electronics, Vol. 51, no. 4, pp. 744–757, August 2004.

[5] T. G. Habetler, F. Profumo, M. Pastorelli, L. Tolbert, **Direct Torque Control of Induction Machines Using Space Vector Modulation.** IEEE Transactions on Industry Applications, Vol. 28, no. 5, pp. 1045–1053, September/October 1992.

[6] J. L. Romeral, A. Arias, E. Aldabas, M. G. Jayne, **Novel Direct Torque Control (DTC) Scheme with Fuzzy Adaptive Torque Ripple Reduction.** IEEE Transactions on Industrial Electronics, Vol. 50, no. 3, pp. 487–492, June 2003.

[7] I. G. Bird, H. Zelaya, **Fuzzy Logic Torque Ripple Reduction for DTC Based AC Drives.** IEE Electronics Letters, Vol. 33, no. 17 August 1997.

[8] J. Kang, S. Sul, **New Direct Torque Control of Induction Motor for Minimum Torque Ripple and Constant Switching Frequency.** IEEE Transactions on Industry Applications, Vol. 35, no. 5, pp. 1076–1082, September/October 1999.

[9] P. Z. Grabowsky, **Direct Flux and Torque Neuro-Fuzzy Control of Inverter Fed Induction Motor Drives.** Thesis. Faculty of Electrical Engineering. Politecnicka Warszawaska, Warsaw University of Technology. 1999.

[10] V. Perelmuter, **Three-Level Inverters with Direct Torque Control.** Industry Applications Conference, pp. 1368–1374, Rome, October 2000.

[11] Z. Tan, Y. Li, Min Li, **A Direct Torque Control of Induction Motor Based on Three-level NPC Inverter.** Power Electronics Specialists Conference, Vol. 3, pp. 1435–1439, June 2001.

[12] K. B. Lee, J. H. Song, I. Choy, J. Y. Yoon, **Improvement of Low-Speed Operation Performance of DTC for Three-Level Inverter-Fed Induction Motors.** IEEE Transactions in Power Electronics, Vol. 48, no. 5, pp. 1006–1014, October 2001.

[13] K. B. Lee, J. H. Song, I. Choy, J. Y. Yoon, **Torque Ripple Reduction in DTC of Induction Motor Driven by Three-Level Inverter with Low Switching Frequency.** IEEE Transactions in Power Electronics, Vol. 17, no. 2, pp. 255–264, March 2002.

[14] Ma A. M. Prats, G. Escobar, E. Galvan, J. M. Carrasco, R. Portillo, **A Switching Control Strategy Based on Output Regulation Subspaces for the Control of Induction Motors Using a Three-Level Inverter.**" IEEE Power Electronics Letters, Vol. 1, no. 2, pp. 29–32, June 2003.

[15] G. Brando, R. Rizzo. **An Optimized Algorithm for Torque Oscillation Reduction in DTC-Induction Motor Drives Using 3-Level NPC Inverter.** in Proc. IEEE International Symposium on Industrial Electronics ISIE04, June 2004, Ajaccio, France, pp. 1215–1220.

[16] J. Rodriguez, J. Lai, F. Z. Peng, **Multilevel Inverters: A Survey of Topologies, Controls, and Applications.** IEEE Trans. on Ind. Elec., Vol 49, no 4, pp. 724–738, August 2002.

[17] A. Nabae, I. Takahashi, H. Akagi, **A New Neutral-Point-Clamped PWM Inverter.** IEEE Transactions on Industrial Applications, Vol. IA-17, no. 5, pages 518–523, Sept./Oct. 1981.

[18] J. C. Trounce, S. D. Round, R. M. Duke, **Comparison by Simulation of Three-Level Induction Motor Torque Control Schemes for Electric Vehicle Applications.** in Proc. International Power Engineering Conference, May 2001, Singapore, pp. 294–299.

Nova shema za izravno upravljanje momentom asinkronih motora napajanih iz trofaznog izmjenjivača. U ovome se članku opisuje novi regulator zasnovan na strategiji izravnog upravljanja momentom i razvijen za primjenu u upravljanju asinkronim motorima napajanim iz trorazinskih izmjenjivača napona. Taj tip izmjenjivača ima nekoliko prednosti u odnosu na standardne dvorazinske izmjenjivače napona, kao što je veći broj razina u izlaznom valnom obliku napona, niži du/dt, manja distorzija harmonika u valnim oblicima napona i struje i niže frekvencije komutacije. U novom regulatoru moment i pogreške u statorskom toku koriste se zajedno s kutnom frekvencijom statora za tvorbu referentne vrijednosti vektora napona. Eksperimentalni su rezultati novog sustava prikazani i uspoređeni s rezultatima klasičnog sustava koji koristi dvorazinski pretvarač napona. Novi regulator pokazuje smanjeni šum u odzivima momenta i toka motora. U predloženom je sustavu također postignuta i manja distorzija struje i manja frekvencija komutacije poluvodičkih sklopova.

Ključne riječi: elektromotorni pogoni promjenljive brzine, izravno upravljanje momentom i tokom, asinkroni motori, višerazinski pretvarači

AUTHORS' ADDRESSES

Xavier del Toro Garcia*, Antoni Arias**, Marcel G. Jayne*, Phil A. Witting*, Vicenç M. Sala**, Jose Luis Romeral**

*   **School of Electronics, University of Glamorgan, Pontypridd, Wales, United Kingdom.**
** **Electronic Engineering Department, Universitat Politècnica de Catalunya, Terrassa, Catalunya, Spain.**